CONTRIBUTION FROM THE MATERIALS SCIENCE LABORATORIES,
DEPARTMENT OF CHEMICAL ENGINEERING, THE UNIVERSITY OF TEXAS AT AUSTIN, AUSTIN, TEXAS 78712

Phase Transitions in Ordered Barium–Rare Earth–Molybdenum Perovskites[1]

BY C. D. BRANDLE AND H. STEINFINK*[2]

Received July 31, 1970

Perovskite-type compounds with the idealized formula $Ba_2LnMo^{V}O_6$ (Ln = La–Lu, Y, Sc) have been prepared. The synthesized materials contain Mo in various oxidation states, usually Mo^{4+}, Mo^{5+}, and Mo^{6+} with the hexavalent state preponderant. The room-temperature crystal structures are orthorhombic for the La and Ce phases, tetragonal for the Pr, Nd, and Sm phases, and face-centered cubic for all other compounds except for Ba_2ScMoO_6 which is hexagonal. The orthorhombic structures have a transition temperature above 1000° to a more symmetric crystal system. The tetragonal phases become cubic above room temperature and the room-temperature cubic phases become tetragonal below room temperature. The transition temperature is a linear function of the rare earth ionic radius and is given by $T(°C) = 2843r_{Ln} - 2769$. The cubic–tetragonal transition is greater than first order and probably of the displacive type. A high-temperature single-crystal X-ray diffraction study on "Ba_2NdMoO_6" has shown that the rare earth ion and molybdenum are ordered in the perovskite structure. The Mo–O distance of 1.86 Å shows that strong covalent bonding is present in this bond, while the Nd–O distance is equal to the sum of the ionic radii.

Introduction

Over the past years many compounds having the perovskite structure have been reported in the literature.[3–5] The ideal perovskite structure for the stoichiometry ABX_3 has a primitive cubic unit cell with space group *Pm3m* containing one formula weight. The mineral itself, $CaTiO_3$, is slightly distorted at room temperature and is orthorhombic, but $SrTiO_3$ displays the ideal structure. The 12- and 6-fold coordinated cation sites, A and B, respectively, can be filled by different ions to produce a general formula $AA'BB'O_6$ and if the octahedral cations, B and B′, order in the structure, then a new ideal face-centered cubic unit cell results which is an integral multiple of the cubic cell. Approximately half of the reported materials have the general formula $A_2BB'O_6$ in which the B and B′ cations order in various degrees in the structure, and distorted supercells belonging to the tetragonal and orthorhombic systems have been reported for these compounds.[6] The compounds selected for detailed study in this investigation have the general formula Ba_2LnMoO_6 (Ln = rare earth). The differences in valence and radius between the B and B′ ions should lead to nearly complete ordering in the structure and the substitution of the various rare earth elements in the B site should provide an excellent means to determine the effect of ionic size on the type of distortion produced in the perovskite structure and the relationship between ionic size and transition temperatures between various structures.

Experimental Section

The rare earth oxides as received from Lindsay Division, American Potash and Chemical Corp., had a reported purity of 99.9%; Sc_2O_3 was obtained from the Atomergic Chemicals Co.; $BaCO_3$ and MoO_3 were of reagent grade purity from the J. T. Baker Co. An X-ray diffraction powder pattern was obtained from the rare earth oxides prior to their use and then several grams of the materials was heated to 1200°, another powder pattern was obtained, and the rest of the material was stored in a desiccator. Only in the case of La_2O_3 was there a considerable weight loss and a change in the diffraction pattern.

The equipment used for reaction of the components was a radiofrequency-heated furnace contained in a bell jar in which the atmosphere was controlled and temperatures in excess of 2000° could be attained. The conditions which gave the best results were a bell jar atmosphere of a nitrogen–12% by volume hydrogen mixture at a pressure of 600 mm. An unconsolidated, powdered sample mixture which contained stoichiometric amounts of Ln_2O_3, MoO_3, and $BaCO_3$ and whose total weight varied between 0.5 and 3 g was heated to 700° and kept at that temperature for 15 min. The temperature was then raised in intervals of 200° up to 1400° with the sample being kept for 15 min at each temperature. The reaction was completed by a final 10-min treatment at 1150° and afterward the sample was permitted to cool to room temperature. This heating schedule and reaction conditions gave single-phase perovskite material in all cases except two. When the compounds Ba_2CeMoO_6 and Ba_2PrMoO_6 were formed, a more strongly reducing atmosphere was necessary; *i.e.*, the hydrogen content was increased from 12 to 20% by volume to obtain a single-phase product. This increase was necessary due to the presence of Ce^{4+} and Pr^{4+} in the initial reactants. The use of an oxidizing atmosphere always resulted in multiple phases; $BaMoO_4$, MoO_3, and Ln_2O_3 were usually detected.

The stoichiometry of the final product was checked by observing the weight loss due to formation of CO_2 and oxygen which occurred in the sample during reaction. The observed weight loss was usually within 1% of the calculated weight loss on the assumption that the reaction was

$$4BaCO_3 + 2MoO_3 + Ln_2O_3 \longrightarrow 2Ba_2LnMoO_6 + 4CO_2 + 0.5O_2$$

Table I compares the values for the observed loss and the theoretical values for several preparations. All observed losses are larger than the theoretical values indicating that some volatilization of MoO_3 occurred.

TABLE I

OBSERVED WEIGHT LOSS IN THE PREPARATION OF "Ba_2LnMoO_6"

	%			%	
Ln^{3+}	Calcd	Obsd	Ln^{3+}	Calcd	Obsd
Y^{3+}	14.73	15.44	Ho^{3+}	13.20	13.75
Ce^{3+}	14.63	16.02	Er^{3+}	13.15	14.33
Pr^{3+}	14.29	15.22	Tm^{3+}	13.11	13.98
Nd^{3+}	13.58	14.86	Yb^{3+}	13.05	13.57
Gd^{3+}	13.33	13.71	Lu^{3+}	13.01	14.06

The compounds as prepared by this procedure are black, have a metallic luster, and are quite crystalline. X-Ray powder patterns showed the diffraction lines of the cubic perovskite subcell in addition to the very weak (111), (311), and (331) superstructure lines due to the ordering of the rare earth and molybdenum ions.

---

[1] This work was sponsored by Grant NSF GK 11376 from the National Science Foundation.

[2] To whom correspondence should be addressed.

[3] A. W. Sleight, J. Longo, and R. Ward, *Inorg. Chem.*, **1**, 245 (1962).

[4] L. Katz and R. Ward, *ibid.*, **3**, 205 (1964).

[5] H. B. Goodenough and J. M. Longo, "Landolt-Börnstein, Numerical Data and Functional Relationships in Science and Technology," K. H. Hellwege, Ed., Group III/Vol. 4a, Springer-Verlag, New York, N. Y., 1970.

[6] A. W. Sleight and R. Ward, *Inorg. Chem.*, **3**, 292 (1964).

To determine the extent of reduction of molybdenum in a series of perovskites, samples of known weight were heated in air at 600° to constant weight and the weight gain was measured using a Cahn Electrobalance with a sensitivity of ±0.02 mg. Sample weights were about 22 mg; *i.e.*, weight changes of greater than 0.1% could be detected. A summary of the results for a set of preparations is shown in Table II. A weight gain of about 1.3% can be expected on the basis of the idealized formula $Ba_2LnMo^VO_6$ for the initial product so that all compounds prepared, except the Gd phase, contained most of the molybdenum in the hexavalent state and the Gd material had primarily tetravalent Mo. On the assumption that the oxidized product contained only Mo^{6+} and that the oxygen framework is retained intact—interstitial oxygen is unlikely—cation vacancies must be present. If the cations are equally exsolved, the final composition can be postulated to have the idealized formula $Ba_{24/18}Ln_{12/18}Mo^{VI}{}_{12/18}O_6$ and the color of the product is most likely due to the color of exsolved rare earth oxide.

TABLE II

WEIGHT CHANGES DURING OXIDATION OF PEROVSKITES WITH PRESUMED COMPOSITION "$Ba_2LnMo^VO_6$"

Ln^{3+}	% gain	Color after oxidn	Ln^{3+}	% gain	Color after oxidn
Nd^{3+}	0.20	Light blue	Tb^{3+}	0.32	Red-brown
Eu^{3+}	0.81	Yellow	Tm^{3+}	0.65	Green-blue
Gd^{3+}	2.43	Yellow	Lu^{3+}	0.56	Green-blue

From these results it is evident that the black material contains several molybdenum oxidation states, the most probable being 4+, 5+, and 6+, and that it will be extremely difficult to predict the composition of a given preparation on the basis of the experimental conditions only. No changes in lattice constants as a function of stoichiometry were observed during this work. The X-ray powder patterns of the oxidized materials are identical with those of the reduced materials except that the diffraction lines of the former were broader and lines in the back-reflection region were quite diffuse.

X-Ray Powder Work

Two distortions of the ideal cubic perovskite structure were observed at room temperature. For the La and Ce compounds, the powder pattern showed splitting of the ideal perovskite lines into triplets which could be indexed on an orthorhombic cell with *a*, *b*, and *c* approximately equal to 8.6 Å. The Pr, Nd, and Sm compounds gave powder patterns which showed the basic perovskite lines being split into either a doublet or a triplet. All lines in the pattern could be indexed on a tetragonal cell with *a* and *c* approximately 8.5 Å. The remaining compounds of Eu through Lu and including Y gave the basic cubic perovskite pattern with no observable line splitting. The Sc compound, however, did not have the perovskite structure but rather the powder pattern was typical of the hexagonal $BaTiO_3$ structure. The room-temperature lattice parameters for the materials as they are initially prepared are given in Table III. These parameters were determined from Debye–Scherrer films obtained with Cu Kα radiation, λ 1.5405 Å, and using a least-squares refinement of all diffraction lines with 2θ angles greater than 90°. The constants for "Ba_2LaMoO_6" could not be obtained because the diffraction lines were broad and the poorly resolved lines did not permit such a refinement. No single crystals of this material were ever obtained.

An X-ray powder diffractometer in which the sample temperature could be varied from 100 to 1400°K was used to study phase changes in these materials. The data from diffraction lines between 34° 2θ and 90° 2θ, Cu Kα radiation, were used in a least-squares refinement to obtain the lattice parameters at various temperatures. The resolution of the instrument placed a lower limit on the observed *c*/*a* ratio of about 1.002. Because of this limitation, powder patterns were run at several different temperatures below the transition temperature. From these patterns, the *c*/*a* ratio was obtained for each material. A linear least-squares fit of the *c*/*a* ratio as a function of temperature, Figure 1, was then performed. This curve was extrapolated to $c/a = 1.0000$ to obtain the transition temperatures which are shown in Table III. It is estimated that the transition temperatures are accurate to ±10° based on the error of the observed *c*/*a* ratio.

TABLE III

LATTICE PARAMETERS, SYMMETRY, AND TRANSITION TEMPERATURES FOR "Ba_2LnMoO_6" MATERIALS[a]

Material	Symmetry	Lattice constants,[b] Å	Transition temp, °C
Ba_2LaMoO_6	Orthorhombic		
Ba_2CeMoO_6[c]	Orthorhombic	$a = 8.52$ $b = 8.74$ $c = 907$	>1000 and <1550
Ba_2PrMoO_6	Tetragonal	$a = 8.495$ (3) $c = 8.597$ (2)	252 (tetragonal → cubic)
Ba_2NdMoO_6	Tetragonal	$a = 8.491$ (4) $c = 8.556$ (4)	176 (tetragonal → cubic)
Ba_2SmMoO_6	Tetragonal	$a = 8.472$ (3) $c = 8.500$ (3)	87 (tetragonal → cubic)
Ba_2EuMoO_6	Cubic	$a = 8.466$ (2)	10 (cubic → tetragonal)
Ba_2GdMoO_6	Cubic	$a = 8.454$ (1)	−16 (cubic → tetragonal)
Ba_2TbMoO_6	Cubic	$a = 8.425$ (2)	−117 (cubic → tetragonal)
Ba_2DyMoO_6	Cubic	$a = 8.409$ (1)	−153[d]
Ba_2YMoO_6	Cubic	$a = 8.391$ (1)	
Ba_2HoMoO_6	Cubic	$a = 8.387$ (1)	−192[d]
Ba_2ErMoO_6	Cubic	$a = 8.369$ (2)	
Ba_2TmMoO_6	Cubic	$a = 8.356$ (2)	
Ba_2YbMoO_6	Cubic	$a = 8.331$ (2)	
Ba_2LuMoO_6	Cubic	$a = 8.321$ (1)	
Ba_2ScMoO_6[c]	Hexagonal	$a = 5.90$ $c = 14.32$	

[a] The numbers in parentheses are the standard deviations of the last digits. [b] Room temperature. [c] Lattice constants obtained from precession films. [d] These values obtained from eq 1.

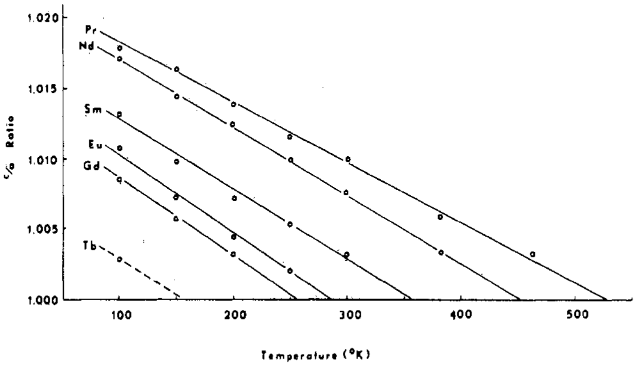

Figure 1.—*c*/*a* ratio *vs.* temperature for tetragonal compounds.

As can be seen from Figure 1, the slope of each of the lines is approximately the same. This fact was used to determine the transition temperature for Ba_2TbMoO_6. For this compound, line splitting (indicating a phase change) was seen only at the lowest possible temperature which could be obtained, 100°K. Using the average of the slopes of the previously determined compounds, a transition temperature of 156°K was calculated from the one datum point.

Examination of the X-ray powder patterns indicated that the change from cubic to tetragonal symmetry occurred with no abrupt change in the lattice parameters, but rather the parameters were a smooth, continuous function of temperature. Figure 2 gives the lattice constants for Ba_2NdMoO_6 as a function of temperature and this behavior is representative for the entire series. Figure 3 shows the volume *vs.* temperature curves for each of the compounds in which phase changes were detected. Within experimental error the curves are linear for each phase; however, the slope of the curve is different for the tetragonal and cubic phases. Except for the compound Ba_2PrMoO_6, the slopes of the curves for the various materials are the same in both the cubic and the tetragonal regions.

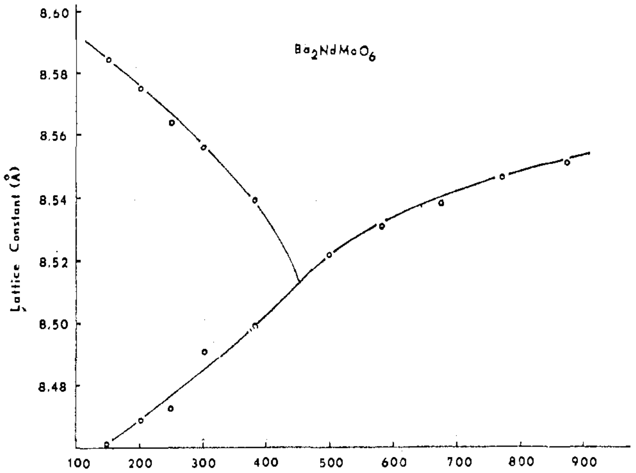

Figure 2.—Lattice constants for Ba_2NdMoO_6 *vs.* temperature. a_C is the cubic value and a_T and c_T are the tetragonal values.

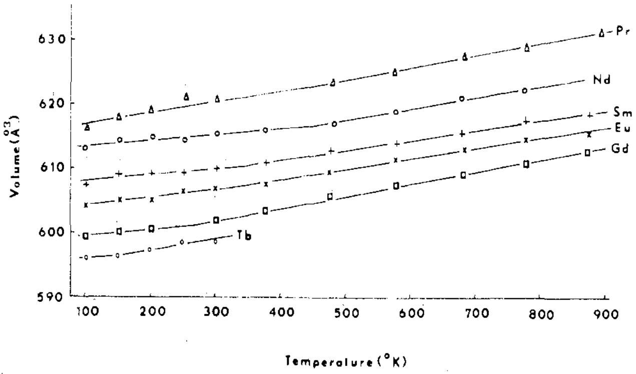

Figure 3.—Unit cell volume *vs.* temperature for tetragonal compounds.

The results indicate that the phase transition is higher than first order. To check this hypothesis further, dta runs were made using samples of Ba_2PrMoO_6 and Ba_2NdMoO_6. In both cases, no evidence of a phase change appeared in the dta charts indicating that the phase transition is higher than first order. Thus it was concluded that (1) the phase change observed in these materials is of the displacive type which results in a gradual displacement of the ions from the high-symmetry position (cubic) and (2) the phase change is higher than first order; *i.e.*, it has no discontinuities in volume, etc., associated with it.

Figure 4 shows the observed transition temperature as a function of the rare earth ionic radius. Within experimental error this curve is linear over the range of materials covered. The expression for the transition temperature as a function of the ionic rare earth radius was obtained by a linear least-squares fit of the data and is given by

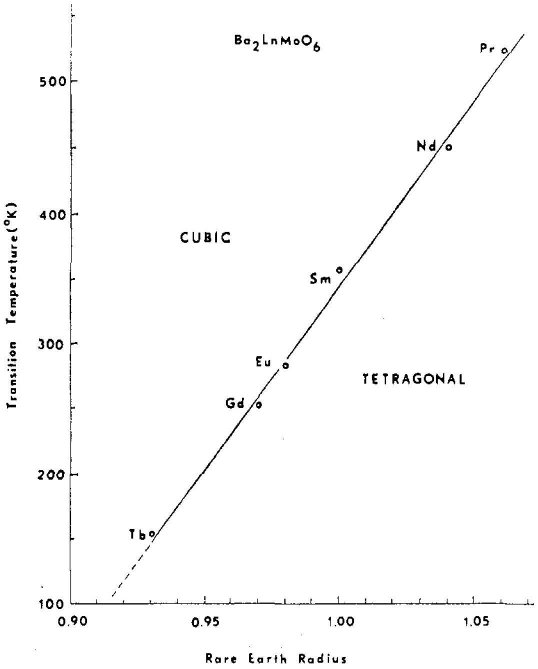

Figure 4.—Transition temperature *vs.* rare earth radius.

$$T = 2843r_{\text{Ln}} - 2769 \qquad (1)$$

where T is the transition temperature (°C) and r_{Ln} is the rare earth ionic radius (Ahren's). This curve was then used to predict transition temperatures for other cubic members of the series. These values are also shown in Table III.

Single-Crystal Studies

In order to study the structures of the various phases and their transitions in greater detail we undertook a single-crystal X-ray diffraction investigation of several materials. Weissenberg and precession photograph patterns were clearly due to twinned crystals. When a high-temperature cubic material transforms to a low-temperature tetragonal phase, the a and c dimensions of which are nearly the same, any one of the original cubic axes can become the new c axis and three possible orientations of the new reciprocal lattices are obtained. Reflections of the types $h00$, $0k0$, and $00l$ (pseudocubic) will appear as doublets and those of the types $h0l$, $0kl$, and $hk0$ will appear as clusters of three. The patterns observed for Ba_2PrMoO_6, Ba_2NdMoO_6, and Ba_2SmMoO_6 at room temperature were of this nature.

To examine the phase transition in greater detail a high-temperature attachment for the Weissenberg camera was constructed. The photographs showed a gradual merging of the diffraction spots as the temperature was increased and above the transition temperature no splitting of the spots was observed. Upon cooling through the transition temperature, splitting of the various diffraction spots was again observed. Cycling through the transition temperature always resulted in the identical twin patterns. Twinning due to phase transitions is a fairly common phenomenon and has been observed in several rare earth aluminates.[7]

Although the room-temperature phase could not be analyzed because of this twinning phenomenon, the high-temperature cubic phase could be investigated by single-crystal X-ray diffraction techniques in order to determine the degree of order that exists in the structure, ensure that it is indeed a perovskite type, and determine the value of the oxygen parameter.

Various flux methods were tried to grow single crystals of Ba_2NdMoO_6 but none were successful and finally the material was melted under a reducing atmosphere in an iridium crucible in the radiofrequency furnace and from the crushed melt a suitable fragment for single-crystal X-ray analysis was obtained.

The crystal was mounted on an automatic equiinclination diffractometer, which was fitted with a device that permitted the heating of the crystal past the transition temperature of 176°. Three-dimensional data to $(\sin\theta)/\lambda = 0.66$ were collected at 200° using crystal-monochromatized Mo Kα radiation. The integrated intensity was measured using an ω scan of 1°/min over a 2.2° scanning range with a counter aperture of 3°. The range was gradually increased to 2.8° for upper levels. A minimum number of counts (2000) was selected to provide the same statistical accuracy for weak reflections as obtained from strong reflections. This procedure required scanning the weak reflections twice. Background was counted for 100 sec on both sides of the peak. Thirteen levels of data were collected (*hk*0–*hk*12) giving a total of 979 reflections. The basis for accepting a reflection as statistically nonzero was a value of $\Delta I/I \leq 0.1$[8] where $\Delta I/I = (T + t^2B)^{1/2}/T - tB$ (T is the total counts in time t_T for the ω scan; B is the total background counts; $t = t_T/(t_1 + t_2)$; t_1 and t_2 are the background counting times). The empirical equation[9]

$$\sigma^2(F) = \frac{F^2}{4(T - B)^2}[T + B + 0.0009(T - B)^2]$$

was used to estimate the variance for each structure factor where T is the total count, B is the average background count, and the additive term $T - B$ allows for errors proportional to the net count, such as variation in the beam intensity and absorption errors. The data were corrected for Lorentz and polarization effects and for absorption. For the absorption correction the crystal, wedge shaped with approximate dimensions 0.096 × 0.024 × 0.103 mm, was described by six planes. The linear absorption coefficient, μ, is 227 cm^{-1} which resulted in transmission factors from about 0.2 to about 0.5. Equivalent reflections were averaged using the standard deviation for the reflection as a weighting function and 115 independent reflections were finally obtained.

High-temperature photographs had shown that reflections were present only when *hkl* were either all even or all odd and that the diffraction symmetry was *m3mF* and the space group of the crystal was therefore assumed to be *Fm3m*. For the initial structure factor calculation a perovskite model was assumed with complete order of the neodymium and molybdenum atoms and the oxygen parameter was assumed to have the ideal value of (¼, 0, 0). Several cycles of least-squares refinement showed that the oxygen parameter shifted from the $^1/_4a_0$ position. Subsequent least-squares refinements based on isotropic temperature factors resulted in a discrepancy value $R = 0.046$ for all reflections used in the refinement and weighted $R = 0.052$ ($R = \Sigma||F_o| - |F_c||/\Sigma|F_o|$ and $wR = \{\Sigma[w(|F_o| - |F_c|)^2]/\Sigma[w|F_o|^2]\}^{1/2}$). The standard deviation for a reflection of unit weight was 3.62. The structure factors were weighted as $1/\sigma^2$ and the quantity $\Sigma w(F_o - F_c)^2$ was minimized with the summation taken over all independent reflections. Atomic scattering factors as listed in ref 10 uncorrected for dispersion effects were used. Table IV lists the observed and calculated structure factors, and final parameters and bond distances for Ba_2NdMoO_6 are shown in Table V. Using the final parameters, a difference map was calculated. Peaks no greater than 0.4 e$^-$/Å^3 were observed and these occurred at the heavy-atom positions Ba and Nd.

TABLE IV

OBSERVED AND CALCULATED STRUCTURE FACTORS FOR Ba_2NdMoO_6

K	L	FOBS	FCAL
***	H =	0	***
0	2	25	18
0	4	748	743
0	6	16	-9*
0	8	454	467
0	10	30	-28
0	12	273	277
0	14	42	-33
2	2	673	682
2	4	18	-16*
2	6	486	499
2	8	22	-38
2	10	321	336
2	12	33	-38
2	14	197	217
4	4	579	585
4	6	23	-23
4	8	411	392
4	10	35	-31
4	12	258	257
6	6	404	404
6	8	30	-35
6	10	294	287
6	12	42	-36
8	8	305	298
8	10	42	-35
8	12	218	210
10	10	216	218
10	12	45	-34
12	12	159	156
***	H =	1	***
1	3	74	70
1	5	35	29
1	7	58	58
1	9	27	38
1	11	39	41
1	13	28	33*
3	3	86	88
3	5	47	46
3	7	64	62
3	9	39	42
3	11	43	42
3	13	27	34*
5	5	27	29
5	7	46	46
5	9	30	36
5	11	38	36
5	13	26	31*
7	7	52	50
7	9	39	39
7	11	39	37
7	13	27	31*
9	9	33	32*
9	11	34	31
9	13	39	27*
11	11	29	29*
***	H =	2	***
2	2	163	-143
2	4	531	554
2	6	49	-68
2	8	413	403
2	10	21	-43
2	12	240	260
4	4	39	-30
4	6	451	440
4	8	28	-39
4	10	308	308
4	12	36	-38
6	6	13	-49*
6	8	335	329
6	10	27	-39
6	12	225	229
8	8	37	-40
8	10	243	246
8	12	43	-37
10	10	39	-36
10	12	185	180
12	12	45	-33
***	H =	3	***
3	3	93	96
3	5	58	57
3	7	68	65
3	9	47	44
3	11	46	42
3	13	27	34
5	5	35	39
5	7	51	49
5	9	33	38
5	11	38	37
5	13	26	31*
7	7	53	51
7	9	39	40
7	11	36	36
7	13	36	30*
9	9	37	33*
9	11	34	31
11	11	27	29*
***	H =	4	***
4	4	507	499
4	6	27	-30
4	8	373	355
4	10	39	-33
4	12	241	239
6	6	374	365
6	8	34	-37
6	10	266	266
6	12	40	-36
8	8	278	276
8	10	42	-35
8	12	201	197
10	10	206	204
10	12	45	-34
***	H =	5	***
5	5	25	29
5	7	38	40
5	9	34	34
5	11	33	33
7	7	42	43
7	9	37	36
7	11	33	33
9	9	32	30*
9	11	24	29*
11	11	29	27*
***	H =	6	***
6	6	19	-41*
6	8	285	283
6	10	36	-37
6	12	201	202
8	8	41	-37
8	10	213	216
8	12	48	-35
10	10	38	-36
10	12	160	160
***	H =	7	***
7	7	39	43
7	9	41	36
7	11	31	32
9	9	36	30*
9	11	27	28*
***	H =	8	***
8	8	214	223
8	10	42	-35
8	12	166	165
10	10	166	170
***	H =	9	***
9	9	31	27*

TABLE V

FINAL PARAMETERS FOR CUBIC Ba_2NdMoO_6, a_0 = 8.518 (1) Å

Atom	Position	x	y	z	B, Å^2
Ba	8c	¼	¼	¼	0.443 (2)
Mo	4b	½	½	½	1.08 (5)
Nd	4a	0	0	0	0.61 (3)
O	24e	0.282 (2)	0	0	4.1 (4)

Bond Distances (Å) for Ba_2NdMoO_6

Nd-O	2.40 (2)
Mo-O	1.86 (2)
Ba-O	3.02 (2)

The determination should provide information regarding the structure type, oxygen parameter, and the degree of order between Nd and Mo. The reflections most sensitive to the last two effects are those with all indices odd, *i.e.*, the superstructure lines. The assumption of complete ordering of Nd and Mo and oxygen in the proper position led to an overall $R = 0.046$. For the superstructure reflections only, R was 0.061. When only the cations were included in the calculation, R was 0.082, and with oxygen included but fixed at the ¼, 0, 0 position, R was 0.069 and a very large temperature

---

[7] S. Geller and V. B. Bala, *Acta Crystallogr.*, **9**, 1019 (1956).

[8] M. Mack, *Norelco Rep.*, **12**, 40 (1965).

[9] W. R. Busing and H. A. Levy, *J. Chem. Phys.*, **26**, 563 (1957).

[10] "International Tables for X-Ray Crystallography," Vol. III, Kynoch Press, Birmingham, England, 1962.

factor was obtained for oxygen. The assumption of 90% order in the perovskite structure yielded $R = 0.066$. Thus a significantly lower discrepancy index was obtained for the complete ordering of the B and B′ ions in the perovskite structure.

Because the high-temperature structure is cubic, there is no distortion of the oxygen octahedra. However, the oxygen octahedra around the rare earth ion and the molybdenum ion are quite different in size. In the former the edge, O–O, is 3.39 Å while in the latter it is 2.63 Å. The oxygen–rare earth bond distance, 2.40 Å, is equal to the sum of the ionic radii of oxygen (1.40 Å) and neodymium (1.00 Å) whereas the oxygen–molybdenum bond distance, 1.86 Å, is about 0.2 Å less than the ionic bond distance, 2.03 Å.[11] Such a short distance would indicate strong covalent bonding between the molybdenum and oxygen atoms and therefore large overlap of the oxygen orbitals and the 4d orbitals of molybdenum. The distance found here corresponds to one of the Mo–O distances observed in $MoO[(S_2COC_2H_5)_2]_2O$[12] and a bond order of about 1.6 can be assigned to it.[13]

The molybdenum radius determined in this compound is 0.46 Å (O_2 radius 1.40 Å), and since the exact oxidation state is unknown, this is an average value for a mixture of the tetra-, penta-, and hexavalent ions. The Mo^{6+} radius in Ba_2CaMoO_6 can be calculated from the lattice constant $a = 8.355$ Å[14] and is 0.38 Å. The Mo^{6+} value is expected to be smaller although it is usually listed as 0.60 Å.[11] In $NaMoF_6$[15] the radius derived for Mo^{5+}, on the basis of the reported lattice constant, $a = 8.194$ Å, $r(Na^+) = 1.02$ Å, and $r(F^-) = 1.33$ Å, is 0.42 Å in closer agreement with the value found here. Perhaps the only conclusion that can be reached is that there is considerable uncertainty regarding the values for Mo radii which can be used, *a priori*, for predicting lattice constants of compounds containing this element.

From the studies of the stoichiometry of these materials it is likely that the single crystal contained Mo^{5+} and Mo^{6+}, and cation vacancies are most likely present in the unit cell. The rather high value of the oxygen temperature factor might be indicative of some disorder in the B sites and provides additional supportive evidence for the postulated nonstoichiometry of these materials.

[11] R. D. Shannon and C. D. Prewitt, *Acta Crystallogr., Sect. B*, **25**, 925 (1969).

[12] A. B. Blake, F. A. Cotton, and J. S. Wood, *J. Amer. Chem. Soc.*, **86**, 3024 (1964).

[13] F. A. Cotton and R. M. Wing, *Inorg. Chem.*, **4**, 867 (1965).

[14] E. G. Steward and H. P. Rooksby, *Acta Crystallogr.*, **4**, 503 (1951).

[15] A. J. Edwards and E. F. Peacock, *J. Chem. Soc.*, 4253 (1961).

CONTRIBUTION FROM THE DEPARTMENTS OF PHYSICS AND CHEMISTRY,
VANDERBILT UNIVERSITY, NASHVILLE, TENNESSEE 37203

π-Bond Feedback Interpreted from the Binding Energy of the "2p" Electrons[1] of Phosphorus

BY WAYNE E. MORGAN, WOJCIECH J. STEC, ROYAL G. ALBRIDGE, AND JOHN R. VAN WAZER*[2]

Received August 26, 1970

The binding energies of the "2p" electrons[1] of phosphorus in 17 compounds were measured by means of X-ray photoelectron spectroscopy. In addition, where appropriate, the binding energies of the "1s" electrons of oxygen, the "2p" electrons of sulfur, and the "3p" electrons of selenium are also reported. The main part of this study involved comparison of the series of compounds having the structure R_3PM, where M stands for (a) the electron pair, (b) oxygen, (c) sulfur, and (d) selenium, with R being the phenyl group and, for structures b through d, the phenoxyl group. In the case of the first series (R = phenyl), data were also obtained on complexes with mercuric iodide. When going from oxygen to sulfur to selenium, there is essentially no change in the "2p"-binding energy and this is attributed to charge equalization through π-bond feedback. Several theoretical calculations, as well as an interpretation of ^{31}P nuclear magnetic resonance chemical shifts, are given to support this contention.

The phenomenon of p_π–d_π bonding has long been a subject of interest and dispute in the chemistry of phosphorus and other second-row elements. X-Ray photoelectron spectroscopy[3–5] of electrons in inner-shell orbitals seems to be a useful tool[3,6] for estimating the variation in the "charge" of an atom from one molecule to another and hence ought to be appropriate for evaluating p_π–d_π bonding. In this work, we shall assume that the inner-electron binding energies obtained from exciting a mass of molecular crystals are at least qualitatively interpretable in terms of the electronic structure of the isolated molecule.[6]

Experimental Section

The photoelectron spectrometer used in this work is a scaled-up version (35-cm radius) of a unit previously described[7] and the operation of the instrument, which is kept in an iron-free room, is controlled by a small computer.[8] This spectrometer has been

---

[1] The designation of the atomic orbital for which a binding energy is measured is put in quotation marks; *e.g.*, "2p," since the inner orbitals of molecules are somewhat delocalized and hence are not identical with the corresponding atomic inner orbitals.

[2] To whom requests for reprints should be addressed.

[3] K. Siegbahn, C. Nordling, A. Fahlman, R. Nordberg, K. Hamrin, J. Hedman, G. Johansson, T. Bergmark, S.-E. Karlsson, I. Lindgren, and B. Lindberg, *Nova Acta Regiae Soc. Sci. Upsal.*, [4] **20**, 1 (1967).

[4] R. G. Albridge in "Physical Methods of Chemistry," Vol. II, A. Weissberger and B. W. Rossiter, Ed., Interscience, New York, N. Y., in press.

[5] J. M. Hollander and W. L. Jolly, *Accounts Chem. Res.*, **3**, 193 (1970).

[6] R. Nordberg, H. Brecht, R. G. Albridge, A. Fahlman, and J. R. Van Wazer, *Inorg. Chem.*, **9**, 2469 (1970).

[7] R. Nordberg, J. Hedman, P. F. Hedén, C. Nordling, and K. Siegbahn, *Ark. Fys.*, **37**, 489 (1968).

[8] A. Fahlman, R. G. Albridge, R. Nordberg, and W. M. LaCasse, *Rev. Sci. Instrum.*, **41**, 596 (1970).